FISEVIER

Contents lists available at ScienceDirect

## Materials Science & Engineering A

journal homepage: www.elsevier.com/locate/msea



## The Portevin–Le Chatelier effect in β-phase Mg–14.3Li–0.8Zn alloy



S.K. Wu a,b,\*, C. Chien b, C.S. Yang a, H.Y. Bor c

- <sup>a</sup> Department of Mechanical Engineering, National Taiwan University, Taipei 106, Taiwan
- <sup>b</sup> Department of Materials Science and Engineering, National Taiwan University, Taipei 106, Taiwan
- <sup>c</sup> Metallurgy Section, Materials and Optoelectronics Research Division, Chung-Shang Institute of Science and Technology, Taoyuan 325, Taiwan

#### ARTICLE INFO

Article history:
Received 9 November 2013
Received in revised form
21 January 2014
Accepted 6 March 2014
Available online 17 March 2014

Reywords:
The Portevin-Le Chatelier effect
Mechanical characterization
Magnesium alloy
Bulk deformation
Plasticity

#### ABSTRACT

The effects of strain rate,  $\dot{\epsilon}$ , and temperature, T, on the occurrence of the Portevin–Le Chatelier (PLC) effect in tensile hot-rolled (HR) and solid-solution treated (SS)  $\beta$ -phase LZ141 magnesium alloy were studied. The HR alloy has an intrinsically higher dislocation density and fewer solute atoms than the SS alloy. This characteristic, in terms of the dynamic strain aging (DSA) mechanism, explains why the PLC effect does not occur in HR alloy for  $\dot{\epsilon}$  ranging from  $3.33 \times 10^{-4} \, \mathrm{s^{-1}}$  to  $6.67 \times 10^{-2} \, \mathrm{s^{-1}}$  but does occur in SS alloy, in which Type B and Type C serrations appear at  $\dot{\epsilon} = (3.33 - 6.67) \times 10^{-3} \, \mathrm{s^{-1}}$  and at  $\dot{\epsilon} = (3.33 - 6.67) \times 10^{-4} \, \mathrm{s^{-1}}$ , respectively. The SS alloy exhibits a negative strain rate sensitivity (SRS) at room temperature. The negative SRS also supports the proposition that the DSA mechanism causes the PLC effect. In the study of the effect of T on the occurrence of the serrated flow, for HR alloy at  $T \le 0$  °C, Type A serrations were observed. In contrast, in the SS alloy, Type C serrations occurred in the curves at 25 °C and 0 °C, and Type B serrations occurred at -25 °C and -50 °C. These results can also be explained by the DSA mechanism. Large serrated stress variations were found in the tensile curves of SS alloy at -25 °C and -50 °C, but no twinning was found near the fractured surface.

 $\ensuremath{\text{@}}$  2014 Elsevier B.V. All rights reserved.

#### 1. Introduction

Mg-Li alloys are less dense than magnesium itself, so they have been the subject of much study in the past. Mg-Li alloys that contain more than  $\approx 11\%$  Li have a single  $\beta$ -phase with a BCC structure, and those that contain  $\approx 5-11\%$  Li consist of two phases,  $\alpha + \beta$ , with the  $\alpha$ -phase having an HCP structure [1–3]. (The composition of the alloy used in this study is given in wt%.) The Portevin-Le Chatelier (PLC) effect, or the so-called "serrated flow", has been reported in  $\alpha$ -phase magnesium alloys. In the 1960s and 1970s, Mg-0.5% Th alloy was reported to have an anomalous yielding effect [4] and serrated flow in the temperature range 240-285 °C [5]. Serrated flow was also observed in Mg-10% Ag alloy at 53–124 °C in solid-solution treated specimens [6,7]. In the past decade, more  $\alpha$ -phase magnesium alloys have been found to exhibit the PLC effect under certain conditions, such as AZ91 (Mg-9% Al-1% Zn) [8], WE54 (Mg-(5.0-5.5)% Y-(1.5-2.0)% Nd-(1.5-2.0)% RE-0.4% Zr) [9], and LA41 (Mg-4.32% Li-0.97% Al) [10]. For Mg-Al-Zn (AZ) alloys, Corby et al. reported that only AZ91 alloy exhibits serrated flow at room temperature [8]. For WE54 alloy, Zhu and Nie [9] observed serrated flow in the temperature range 150–225 °C and attributed it to the dynamic strain aging (DSA) effect [11]. For LA41 alloy containing <5% Li, Wang et al. [10] found that serrated flow is apparent throughout the tensile deformation and that this alloy exhibits abnormal strain rate sensitivity (SRS), with SRS being positive in the strain rate ( $\dot{\epsilon}$ ) range  $1.33\times10^{-4}$ –6.67  $\times10^{-4}$  s $^{-1}$ , and negative in the  $\dot{\epsilon}$  range  $6.67\times10^{-4}$ –1.33  $\times10^{-2}$  s $^{-1}$ . The variation in SRS is thought to result from competition between the DSA of solute atoms and the shearing of precipitation by dislocations.

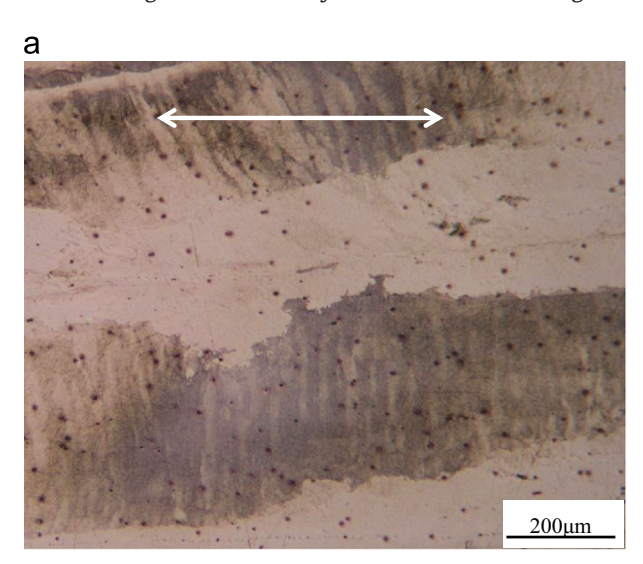
Many studies have been focused on Mg–Li β-phase alloys that contain more than 12% Li because of their intrinsic ultralight property. Clark and Sturkey reported that, for Mg–19.5Li–18.7Zn alloy aged at 21–150 °C, a transition structure  $\theta$  (MgLi<sub>2</sub>Zn) phase is generated upon precipitation of the stable LiZn phase, which is observed in the Debye–Scherrer X-ray pattern [12]. Levinson and McPherson studied Mg–12.3Li–1.0Al alloy and found that  $\theta$  (MgLi<sub>2</sub>Al) phase is not an equilibrium phase in the temperature range 100–400 °C [13]. Takuda et al. studied tensile Mg–12Li–1Zn alloy and found it is particularly sensitive to  $\dot{\varepsilon}$  and has sufficiently high ductility at low  $\dot{\varepsilon}$  [14]. Song et al. reported that, for Mg–12Li–0.03Be–xAl (x=1, 3) alloys, the  $\theta$  phase is formed at room temperature in the casts, and its formation is accelerated if the Al content is increased [15]. Liu et al. studied equal channel angular processed (ECAP) Mg–14Li–1Al (LA141) alloy and found that the grains of the  $\beta$ -phase matrix are substantially more

<sup>\*</sup> Corresponding author at: Department of Materials Science and Engineering, National Taiwan University, No. 1, Sec. 4, Roosevelt Road, Taipei 106, Taiwan. E-mail address: skw@ntu.edu.tw (S.K. Wu).

refined [16]. Wu et al. studied the mechanical properties of cold-rolled and/or solid-solution treated  $\beta$ -phase Mg–14.3Li–0.8Zn (LZ141) alloy and concluded that the duplex strengthening effect of solid-solution and subsequent severe cold-rolling significantly improves the mechanical properties [17]. Studies of  $\beta$ -phase Mg–Li alloys tend to focus on aspects such as their microstructural observation, the  $\theta/\theta$  phase transition, and their mechanical properties. Although the PLC effect has been observed in iron (BCC structure) containing small concentrations of carbon [18], the PLC effect in tensile deformed  $\beta$ -phase Mg–Li alloys has not yet been reported. In this study, the PLC effect was exhibited in the tensile stress–strain curves of  $\beta$ -phase Mg–14.3Li–0.8Zn (LZ141) alloy. The effect of  $\dot{e}$  and temperature on the occurrence of the PLC effect and the reasons for this phenomenon are discussed.

#### 2. Experimental procedures

LZ141 alloy was prepared from the pure raw materials of magnesium (purity 99.95%), lithium (purity 99.9%), and zinc (purity 99.99%). These raw materials were induction-melted and protected by argon gas, cast in a steel mold, and homogenized at 350 °C for 12 h. The optical micrograph (OM), X-ray diffraction (XRD) pattern and scanning electron microscope (SEM) image of as-homogenized LZ141 alloy were shown in our previous work [17]. The precise chemical composition of as-homogenized LZ141 alloy was determined to be Mg–14.3Li-



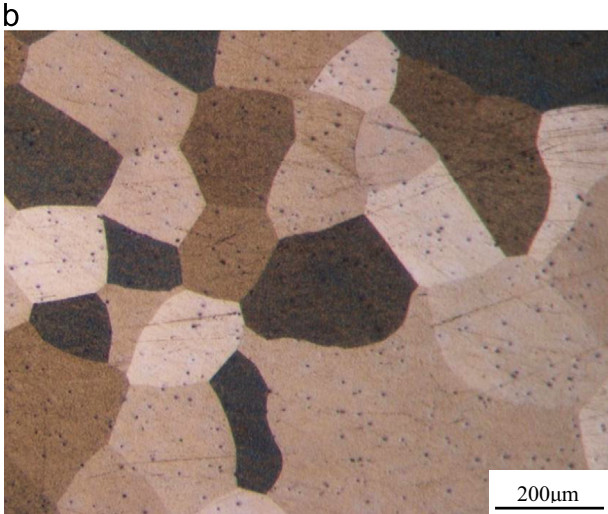


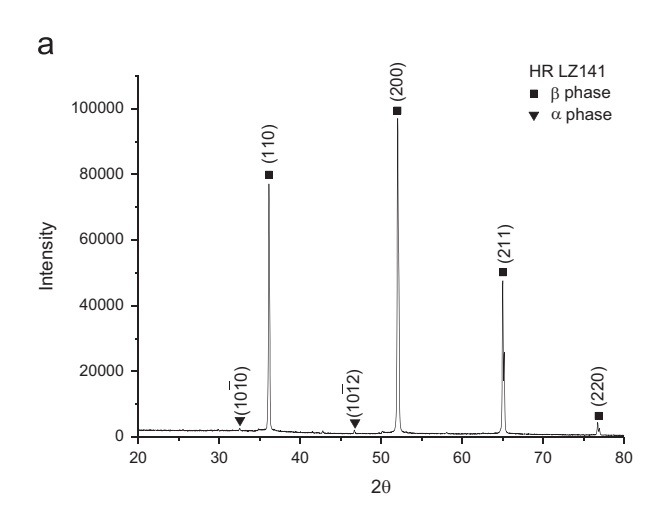
**Fig. 1.** Optical micrographs of (a) hot-rolled (HR) and (b) solid-solution treated (SS) LZ141 alloys. The arrow shown in (a) is the rolling direction.

0.8Zn, with trace amounts of Al, Mn and Fe of less than 0.02%, using an inductively coupled plasma-optical emission spectrometer (ICP-OES). The homogenized ingot was sliced into plates of 30 mm thickness. The plates were then hot-rolled (abbreviated as HR) at 200 °C to plates thickness of 3 mm. The specimens for solid solution treatment (abbreviated as SS) were HR allov heated to 350 °C for 20 min and then water-quenched. The specimens for microstructural examination were prepared using the standard metallographic procedure with an etching solution of 1 ml 2,4,6-trinitrophenol, 1 ml water, and 7 ml ethanol. Microstructural observations were performed using a Nikon optical microscope. The ASTM E112-88 standard was used to calculate the average grain size [19]. The specimens for tensile tests were produced according to ASTM E8/E8M-13a [20] with a gauge length of 25.0 mm and width of 6.0 mm. Tensile tests were performed using a Shimadzu testing machine (AG-IS 50 kN, Japan) with a stroke control and a strain rate  $\dot{\varepsilon}$  of  $6.67 \times 10^{-5}$ – $6.67 \times 10^{-2}$  s<sup>-1</sup>. XRD measurements of the crystal structure were performed using a Rigaku diffractometer (Rigaku TTR AXIII, Japan) with a Cu  $K_{\alpha}$  X-ray tube operated at 50 kV voltage and 300 mA current at a step width of  $0.02^{\circ}$ and a measurement time of 0.3 s per step.

#### 3. Results and discussion

#### 3.1. Microstructure observation and XRD measurement

Fig. 1(a) and (b) shows OM images of HR and SS LZ141 alloys on the rolling plane, respectively. Fig. 1(a) demonstrates that the



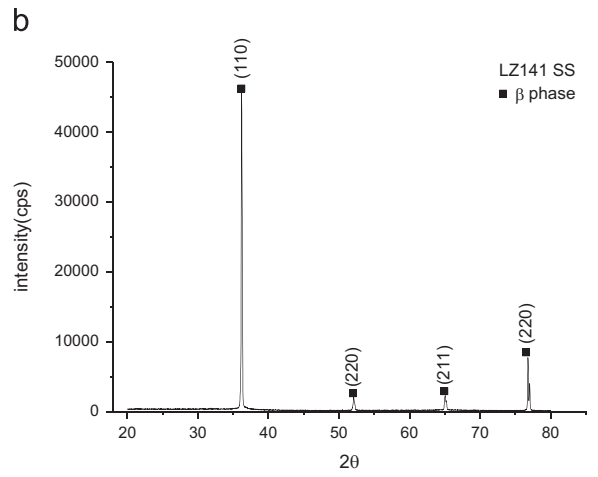


Fig. 2. X-ray diffraction (XRD) patterns of (a) hot-rolled (HR) and (b) solid-solution treated (SS) LZ141 alloys.

### Download English Version:

# https://daneshyari.com/en/article/1575179

Download Persian Version:

https://daneshyari.com/article/1575179

<u>Daneshyari.com</u>